An alternative theory on relaxation rates in cuprate superconductors

2009 J. Phys.: Condens. Matter 21 025701

(http://iopscience.iop.org/0953-8984/21/2/025701)

J. Phys.: Condens. Matter **21** (2009) 025701 (10pp) doi:10.1088/0953-8984/21/2/025701

An alternative theory on relaxation rates in cuprate superconductors

Nie Luo and George H Miley

Department of Nuclear, Plasma, and Radiological Engineering, University of Illinois, Urbana, IL 61821, USA

E-mail: nluo@uiuc.edu

Received 5 June 2008, in final form 7 November 2008
Published 11 December 2008
Online at stacks.iop.org/JPhysCM/21/025701

Abstract

Transport properties of high transition temperature (high-T_c) superconductors *apparently* demonstrate two distinct relaxation rates in the normal state. We propose that this superficial inconsistence can be resolved with an effective carrier (quasiparticle) density n almost linear in temperature T. Experimental evidence both for and against this explanation is analyzed and we conclude that this offers a clear yet promising scenario. Band structure calculation was utilized to determine the Fermi surface topology of the cuprate superconductor versus doping. The results demonstrate that an electron-like portion of the Fermi surface exists in a wide range of doping levels even for a p-type superconductor, exemplified by $La_{2-x}Sr_xCuO_{4-\delta}$ (LSCO). Such electron-like segments have also been confirmed in recent photoemission electron spectroscopy. The Coulomb interaction between electron-like and hole-like quasiparticles then forms a bound state, similar to that of an exciton. As a result the number of charge carriers upon cooling temperature is decreased. A quantum mechanical calculation of scattering cross section demonstrates that a T^2 relaxation rate is born out of an electron–hole collision process. Above the pseudogap temperature T^* the normal state of high-T_c cuprates is close to a two-component Fermi liquid. It, however, assumes non-Fermi-liquid behavior below T^*.

(Some figures in this article are in colour only in the electronic version)

1. Introduction

The peculiar normal-state transport properties of high-T_c superconductors are rather controversial and not well understood. The most striking of these is the observation of the so-called two relaxation rates [1]. The resistivity ρ is linear in temperature T for optimally doped samples [2], which implies a transport (longitudinal) relaxation rate $1/\tau_{tr} \propto T$ from $\rho = m_c/ne_c^2\tau_{tr}$ assuming that e_c, m_c and n, respectively the charge, mass and density of carriers, are T-independent. In contrast, the Hall (transverse) relaxation rate $1/\tau_H$ from the cotangent of the Hall angle $\cot\theta_H = m_c c/e_c H\tau_H$ is essentially quadratic in T. These two distinct T dependences have various explanations. A widely known one is due to Anderson, based on the spin–charge separation scenario of the Luttinger liquid [1]. Other interesting schemes include, but are not limited to, the near-antiferromagnetic Fermi liquid (NAFL) theory of Pines *et al* [3] and marginal Fermi liquid (MFL) theory by Varma *et al* [4], to name a few.

We are here to point out that the two distinct rates might be superficial if the effective carrier density (concentration) n actually depends on T or $n = n(T)$. Especially if the $n(T) \propto T$, then we are left with perhaps only one rate, for both longitudinal and transverse processes. This is easy to see because $1/\tau_{tr} = n(T)e_c^2\rho/m_c$ (in Gaussian units) and as long as $n(T) \propto T$ and $\rho \propto T$ we then get $1/\tau_{tr} \propto T^2$. It has therefore the same T dependence as $1/\tau_H$ from the Hall effect.

Similar explanations have been proposed before [5–7]. Alexandrov and Mott also suggest $n(T) \propto T$ although their carriers are bosons (bipolarons) [8, 9]. Levin and Quader [10] advocate a model where non-degenerate and degenerate carriers possess two different relaxation rates. The density of the non-degenerate carriers is determined by various thermal activation processes. Therefore the overall carrier density is T-dependent, albeit *not necessarily* linear in T. More recently, a similar model was studied in detail by Gor'kov and Teitel'baum [11, 12] and the authors specifically attributed the T-dependent component to exciton-like bound

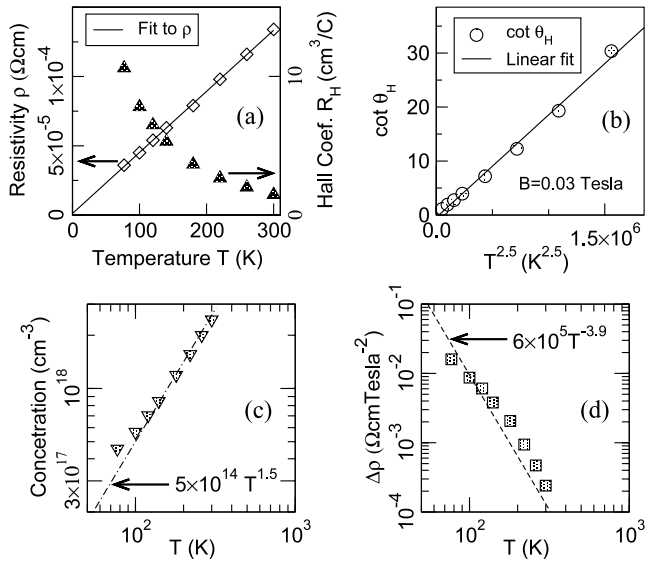

Figure 1. (a) Resistivity ρ (ρ_{33}) and Hall coefficient $R_{\rm H}$ (R_{231}) versus T in Bi after [14]. (b) $\cot\theta_{\rm H}$ versus $T^{2.5}$ calculated from ρ_{33} and $R_{\rm H}$ (R_{231}). (c) Concentration for both electron and hole versus T. (d) Magnetoresistance $\Delta\rho$ (A_{33}) versus T.

states, in a striking similarity to the scheme proposed here. This notion of a variable n, however, does not come without some (often superficial) difficulties. For example, optical conductivity seems to suggest that spectral weight of the Drude part is independent of T [13–15], implying a constant n. Nevertheless, we will show later that such an evidence is oversimplified.

2. Relaxation rates in transport

Although the discrepancy between $\rho \propto T$ and $\cot\theta_{\rm H} \propto T^2$ is often treated as abnormal in the high-$T_{\rm c}$ world, similar behaviors happen elsewhere, typically in some semi-yet traditional metals, where a single relaxation rate dominates transports. Therefore, such a discrepancy is not limited to cuprates. One question is naturally raised, that is, do $\rho \propto T$ and $\cot\theta_{\rm H} \propto T^2$ really indicate two relaxation rates? A number of theories exist but a general consensus is not reached yet. Nevertheless recent and refined experiments seem to indicate a single rate, as we will discuss later.

2.1. Relaxation rate in semimetals

Bismuth displays a similar discrepancy from 77 to 300 K as shown in figures 1(a) and (b), although with a $\cot(\theta_{\rm H}) \propto T^{2.5}$ instead [16][1]. This behavior has long been understood from a single rate $1/\tau \propto T^{2.5}$ and a variable $n(T) \propto T^{1.5}$ (see figure 1(c)), which in combination give a $\rho \propto T$. It is very *unlikely* that a Luttinger liquid theory is relevant to a three-dimensional conductor, to which Bi belongs. Then, taking such a discrepancy as the evidence for spin–charge separation does not seem to be convincing.

[1] Michenaud confirmed to the author that tick mark labels for the vertical axis of figure 2 should be 10^{-7}, 10^{-8} and 10^{-9} downwards. Data are from table 2.

With a much lower n ($\sim 10^{17}$ cm^{-3}), the semimetal Bi still has a lower resistivity than most cuprates in their normal states, which are often treated as metals. This raises the question of whether doped cuprate is a metal, a semimetal or even a semiconductor, as suggested by Alexandrov and Mott [9, 17]. We believe that it has characters of all three. It is like a metal or semimetal as required by a non-zero n when approaching 0 K. On the other hand, significant electrostatic field effects on the transport [18], the divergent 0 K resistance under a strong magnetic field [19] and the likely variable n from the Hall effect [20] put it near semiconductors and semimetals, quite far from a simple metal[2] where n is taken as fixed.

2.2. The case of cuprates

Let us go back to other evidence supporting the $n(T) \propto T$ argument. First and foremost is actually the Hall coefficient $R_{\rm H}$ itself. Within the temperature range where $\cot\theta_{\rm H} \propto T^2$, $R_{\rm H}$ can be nicely fitted by $1/(a_0 + a_1 T)$ in optimally doped (OD) p-type cuprates [20]. Such a fit is even upheld in recent infrared Hall experiments at a high energy scale of $\approx$0.1 eV [21]. Note that $R_{\rm H} = 1/ne_{\rm c}c$ or equivalently $1/e_{\rm c}cR_{\rm H}$ measures n in a simple parabolic band. However, a naive explanation of $n = 1/e_{\rm c}cR_{\rm H}$ seems not prudent because $R_{\rm H}$ may reach 0 in some cuprates. This is perhaps why the T-dependent $R_{\rm H}$ is not widely accepted as evidence for $n(T) \propto T$. However, $R_{\rm H} = 0$ can be understood with a two-carrier model as a result of compensation [23–27]. And as long as one carrier dominates the transport, $R_{\rm H}$ is still $\propto 1/n$ although $e_{\rm c}cR_{\rm H} = 1/n$ no longer holds. To see this, suppose that the densities of two carriers are given respectively by $n_{\rm e} = n_{\rm e0} + n_{\rm e1}T$ and $n_{\rm h} = n_{\rm h0} + n_{\rm h1}T$, giving rise to a Hall coefficient

$$R_{\rm H} = \frac{n_{\rm h} - n_{\rm e}b^2}{e_{\rm c}c(n_{\rm h} + n_{\rm e}b)^2} = \frac{(n_{\rm h0} - n_{\rm e0}b^2) + (n_{\rm h1} - n_{\rm e1}b^2)T}{e_{\rm c}c[(n_{\rm h0} + n_{\rm e0}b) + (n_{\rm h1} + n_{\rm e1}b)T]^2},$$

where $b = \mu_{\rm e}/\mu_{\rm h}$ is the mobility ratio. If $n_{\rm e1}T \gg n_{\rm e0}$, $n_{\rm h1}T \gg n_{\rm h0}$ and $n_{\rm h1} - n_{\rm e1}b^2 \neq 0$, $R_{\rm H}$ is roughly $\propto 1/T$. Thus the Hall effect strongly suggests $n(T) \propto T$ in the normal state of OD p-type cuprates[3].

$R_{\rm H}$ is arguably the most widely used and quite accurate method to determine n in metals and semiconductors when compensation is not severe. It is not persuasive to treat one-half of the Hall effect, say $\cot\theta_{\rm H} \propto T^2$ as exact, while disregarding the physical meaning of the other half, namely $R_{\rm H} \propto 1/T$, for $\cot\theta_{\rm H} = m_{\rm c}c/e_{\rm c}H\tau_{\rm H}$ itself holds strictly only for a simple parabolic band, just as $R_{\rm H} = 1/ne_{\rm c}c$. Actually, putting these two facts on an equal footing makes the physics compact and concise: there roughly exists a relaxation rate $1/\tau \propto T^2$, governing both longitudinal and transverse processes. $\rho = m_{\rm c}/n(T)e_{\rm c}^2\tau_{\rm tr} \propto T$ is the result of $1/\tau_{\rm tr} \approx 1/\tau \propto T^2$ and $n(T) \propto T$, while $\cot\theta_{\rm H} = m_{\rm c}c/e_{\rm c}H\tau_{\rm H}$ has no $n(T)$ in it, thus

[2] n from $R_{\rm H}$ is nearly constant for group IA metals like Na, K and noble metals (100 K $< T <$ 350 K, where $\rho \propto T$). n may vary even for some metals like Al, because of its sizable $R_{\rm H}$ dependence on T. Certainly the variation in $R_{\rm H}$ cannot come from n only. See, for example, [22].

[3] It is better to write $n(T) = a + bT$ instead of $n(T) \propto T$. We, however, generally neglect the difference in two such notations for the sake of simplicity.

$\cot\theta_H \propto 1/\tau_H \approx 1/\tau \propto T^2$. (We assume that m_c is relatively T-independent and this issue will be addressed later.) With a non-fixed n, we can proceed to see that the apparent violation of Kohler's rule [28] is actually superficial.

2.2.1. Kohler's rule. Kohler's rule in its ordinary form states that the relative magnetoresistance $\Delta\rho/\rho_0$ in a magnetic field H can be represented in the form [29]

$$\Delta\rho/\rho_0 = F(H/\rho_0), \tag{1}$$

where ρ_0 is the resistivity at $H = 0$ and F is a function given by the metal and its sample geometry only.

In cuprates, approximately [28] $\Delta\rho/\rho_0 \propto H^2T^{-4}$ but $H/\rho_0 \propto HT^{-1}$. Because $\Delta\rho/\rho_0$ (or H^2T^{-4}) is not a function of H/ρ_0 (or HT^{-1}) only, Kohler's rule *seems* to be violated.

The argument above is, however, not valid if carrier (or alternatively referred to as quasiparticle) density n is not fixed. A scrutiny of its derivation [29] shows that a more general form of Kohler's rule is

$$\Delta\rho/\rho_0 = F(H\tau), \tag{2}$$

where τ is the single relaxation time assumed for that conductor. For simple metals, n is roughly a constant, so that τ has the same T dependence as ρ_0 and thus there is no problem if one writes $\Delta\rho/\rho_0 = F(H/\rho_0)$ instead of $F(H\tau)$. However, for cuprates, n likely depends on T, so we should use equation (2) instead of equation (1) in order to see if Kohler's rule survives. Because $H\tau \propto HT^{-2}$, where $1/\tau$ is the single rate assumed, we have $\Delta\rho/\rho_0 \propto H^2T^{-4} = (HT^{-2})^2$ and thus $\Delta\rho/\rho_0 \propto (H\tau)^2 = F(H\tau)$ so that Kohler's rule still holds. Similarly in Bi, $\Delta\rho/\rho_0 \propto H^2T^{-5} = (HT^{-2.5})^2$ inferred from figure 1(d) and so we get $\Delta\rho/\rho_0 \propto (H\tau)^2 = F(H\tau)$ because $1/\tau \propto T^{2.5}$ here in Bi. Kohler's rule is not violated either. A thorough derivation and analysis was given by the authors elsewhere [30].

The perseverance of Kohler's rule barely strengthens the idea of a single rate $1/\tau \propto T^2$. Thus our previous explanation of the Hall effect seems to be in the right direction. Angle-resolved photoemission spectroscopy (ARPES) studies also suggest the applicability of semimetal band structure to cuprates. Figure 2 shows some likely scenarios how this might be materialized in Bi-2212 with the two-dimensional Fermi surface (FS) mapping following [28]. The discussion can be generalized to other p-type superconductors. Note that the discussion here represents the FS understanding of some seven years ago, but is nevertheless published here to serve as a historical perspective. More recent studies have improved our understanding and answered some puzzling questions outlined in figure 2. These will be discussed in the later part of the paper.

2.2.2. Mid-infrared. Having mentioned some evidence for the single-rate explanation, we now discuss experiments still at odds with it. The apparently most serious one, in our opinion, is from the optical conductivity $\sigma(\omega)$. To account for the non-Drude behavior of $\sigma(\omega)$ in cuprates, a classical two-component model [32] is used in quite a few studies:

$$\sigma(\omega, T) = \sigma_D(\omega, T) + \sigma_{MIR}(\omega, T), \tag{3}$$

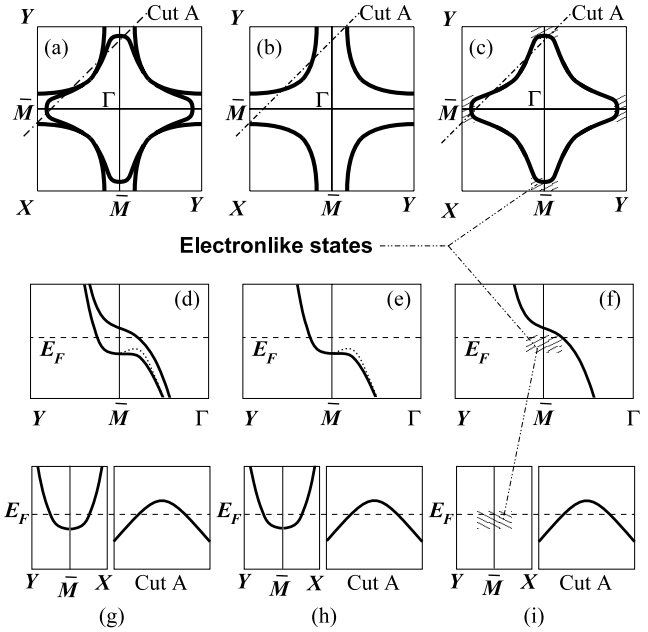

Figure 2. 2D Fermi surface and band structure scenarios of generic cuprate superconductors from ARPES. (a) FS due to split from two CuO_2 planes. (b) Hole-like FS shared by all cuprates. (c) Hole-like FS with electron-like states shown as the shaded area. (d)–(f) Band structures near FS along Y–M̄–Γ for cases shown in (a)–(c) (see footnote 3). Dotted lines along M̄–Γ in (d) and (e) indicate hypothesized band dispersion which stabilizes local minimum at M̄. (g) The lower band of (d) unfolded along Y–M̄–X in the left panel. The band is electron-like near M̄ along Y–M̄–X. (h) Band of (e) unfolded along Y–M̄–X in the left panel, electron-like. (i) Electron-like states near M̄ in the left panel. The right panels of (g)–(i) show hole-like band dispersion near $(\pi/2, \pi/2)$ along Cut A, indicated by dashed–dotted lines in (a)–(c). The possible complication in hole-like bands from the bilayer splitting near $(\pi/2, \pi/2)$ as in (a) is neglected. E_F is the Fermi level in all cases. The Brillouin zone notation is that often adopted for Bi-22$(n-1)n$ systems. With slight modification, the pictures depicted here can be adopted for superconductors of space group $I4/mmm$, such as $La_{2-x}Sr_xCuO_{4-\delta}$.

where $\sigma_D(\omega, T) = [n(T)e_c^2/m_c]\{(1/\tau)/[\omega^2 + (1/\tau)^2]\}$ is the T-dependent Drude part while $\sigma_{MIR}(\omega, T)$ is the *nearly* T-independent mid-infrared (MIR) part. The spectral weight of the Drude part, $\int_0^\infty \sigma_D(\omega, T)\,d\omega$, is found to be independent of T (the shape of $\sigma_D(\omega, T)$ is T-dependent though), suggesting a constant n if m_c is taken independent of T. Nonetheless the typical use of such a model is oversimplified. The problem is: the MIR is treated as T-independent and modeled as classical Lorentz oscillators.

The T dependence of MIR is tied to its nature. MIR is often understood as an interband electronic transition [33, 34]. This interband transition, especially at its low ω part, is, however, not from excitation over the charge-transfer (CT) gap. Rather, it perhaps comes from doping-related states and spectral weight transfers inside the CT gap as suggested by various doping-dependent photoemission, inverse photoemission, x-ray absorption, electron-energy-loss spectroscopy and IR reflectance studies [35, 34]. Without lingering over the exact origin of these MIR-related states, we have two observations from experiments. First, MIR states

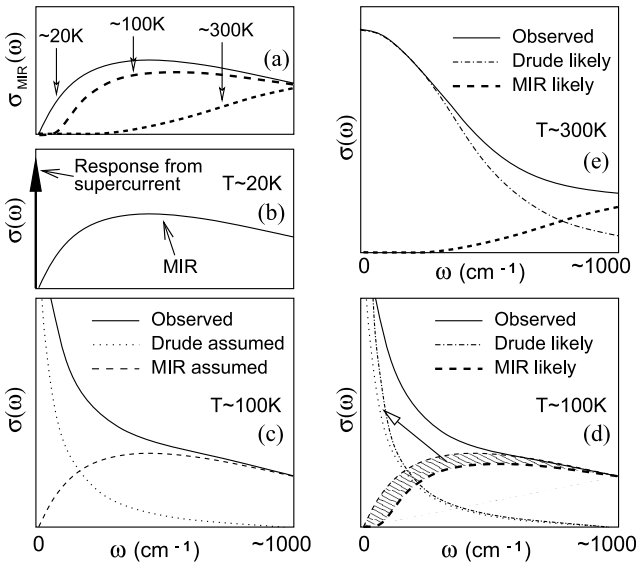

Figure 3. Spectral weight transfer between the Drude and MIR parts of optical conductivity $\sigma(\omega, T)$ in cuprates. (a) Theoretical variation of $\sigma_{\rm MIR}(\omega, T)$ with T in a quantum model. (b) The $\sigma(\omega)$ as found at 20 K. (c) $\sigma(\omega)$ at ∼100 K. The dashed line is the $\sigma_{\rm MIR}(\omega, T)$ assumed in the typical two-component analysis, which is the same as $\sigma_{\rm MIR}(\omega)$ at 20 K. The dotted line is the calculated $\sigma_{\rm D}(\omega)$ by using $\sigma(\omega, 100\ {\rm K}) - \sigma_{\rm MIR}(\omega, 20\ {\rm K})$. (a)–(c) share the same horizontal axis. (d) $\sigma(\omega)$ at ∼100 K. The thick dashed line is the actual $\sigma_{\rm MIR}(\omega)$ at 100 K as shown in (a) as the long dashed line. The dashed–dotted line is the actual $\sigma_{\rm D}(\omega)$ at 100 K by using $\sigma(\omega, 100\ {\rm K}) - \sigma_{\rm MIR}(\omega, 100\ {\rm K})$. The thin dashed and dotted lines are the same as those in (c) for comparison. Obviously the Drude weight obtained in (d) is larger than that in (c), which means an higher carrier density at 100 K compared with 20 K. The shaded area is the spectral weight transferred away from MIR as indicated by the arrow when T reaches 100 from 20 K. (e) $\sigma(\omega)$ at ∼300 K. The spectral weight of MIR is further transferred to the Drude part.

are very close to the Fermi level, manifested by a low energy MIR tail approaching $\omega = 0$.[4] Such states might relate to the flat band, van Hove singularity and electron-like states (see figures 2(c) and (f)) revealed in ARPES. Second, MIR states are localized at low T as seen in $\sigma(\omega)$ at 20 K or lower [13, 14] as shown in figure 3(b), because otherwise it would behave Drude-like and there would not be an MIR at all. Then the interband transitions of MIR are likely from shallow localized states to extended ones. Later we will show how strong correlation combined with the peculiar band structure of cuprates might contribute to the localized state.

With these two properties of MIR states, $\sigma_{\rm MIR}$ should be T-dependent in its low ω part (actually in the far-infrared, FIR), because higher T should progressively set more carriers free, which corresponds to a spectral weight transfer from MIR (or FIR) to the Drude part, as indicated by the arrow in figure 3(d). In other words, the classical model of Lorentz oscillator with a T-independent MIR is *not* correct considering the quantum nature of interband excitations. With increasing T, there should be a reduction in the spectral weight of MIR as shown in figure 3(a), and this reduction in MIR should then be made up by an increase in the Drude part (figure 3(d)) according to the sum rule (i.e. a spectral weight transfer). Such weight reduction [36] and weight transfer [37] have been understood in optical studies of narrow-gap semiconductors like HgTe, $Hg_{1-x}Cd_xTe$ and semimetals such as Bi. Unlike the valence-to-conduction-band type of transition there ($\Gamma_8 \rightarrow \Gamma_8$ in HgTe, $Hg_{1-x}Cd_xTe$ and possibly crossing the L-point gap in Bi), the MIR in cuprates are likely from localized to extended bands, but a similar T dependence should still hold. However, being overlapped $\sigma_{\rm D}$ and $\sigma_{\rm MIR}$ in cuprates have no clear-cut method to separate. (Overlap of the two parts in $Hg_{1-x}Cd_x$ Te and Bi is not as severe.) So what is often used in analysis is assuming that the $\sigma_{\rm MIR}$ at 20 K or lower, written indiscriminately as $\sigma_{\rm MIR}(\omega, 20\ {\rm K})$ for simplicity, be the same for all other T [13, 14]. Such a procedure, without little doubt, would make a constant Drude weight simply because of the conductivity sum rule.

Rewrite equation (3) as

$$\sigma_{\rm D}(\omega, T) = \sigma(\omega, T) - \sigma_{\rm MIR}(\omega, T). \tag{4}$$

Integrate both sides over ω from 0 to ∞, and by using a sum rule for $\sigma_{\rm D}(\omega, T)$, we get

$$\frac{\pi n(T) e_{\rm c}^2}{2m_{\rm c}} = \int_0^\infty \sigma(\omega, T)\,{\rm d}\omega - \int_0^\infty \sigma_{\rm MIR}(\omega, T)\,{\rm d}\omega, \tag{5}$$

where the total weight $\int_0^\infty \sigma(\omega, T)\,{\rm d}\omega$ of the two parts basically measures the number of states available within the CT gap[5]. It is directly integrated from experimental $\sigma(\omega, T)$ and is found independent of T. If a $\sigma_{\rm MIR}(\omega, T) = \sigma_{\rm MIR}(\omega, 20\ {\rm K})$ is assumed for all T, as is done in a typical T-dependent two-component analysis [13, 14], we are left with

$$n(T) = \frac{2m_{\rm c}}{\pi e_{\rm c}^2}\left[\int_0^\infty \sigma(\omega, T)\,{\rm d}\omega - \int_0^\infty \sigma_{\rm MIR}(\omega, 20\ {\rm K})\,{\rm d}\omega\right]. \tag{6}$$

Because $\int_0^\infty \sigma_{\rm MIR}(\omega, 20\ {\rm K})\,{\rm d}\omega$ is a constant, the right-hand side of equation (6) is T-invariant, and we are left with an effective carrier density $n \propto \int_0^\infty \sigma(\omega, T)\,{\rm d}\omega - \int_0^\infty \sigma_{\rm MIR}(\omega, 20\ {\rm K})\,{\rm d}\omega$, which is independent of T even if n changes with temperature in reality. The introduction of self-consistent iteration [14] marginally improves the result but qualitatively it would not cure the problem. There are different approaches using straightforward least-squares fit [14, 15]. However, with a classical and oversimplified Drude–Lorentz model to start from, such fits are not likely to uncover the sizable T dependence of the Drude weight.

Meanwhile the high ω part of MIR is less affected by T, as easily understood from quantum statistics and because the MIR is several times larger than the Drude part, a spectral transfer of the order of one Drude weight does not contradict the convention of nearly T-independent MIR. The transfer only occurs at low ω where the overlap with the Drude peak makes its detection hard.

The analysis above explains the origin of variable n as well: as T increases, previously localized carriers are now

[4] The low energy tail of MIR often extends down to ∼100 $\rm cm^{-1}$, and sometimes extrapolates to $\omega \approx 0$.

[5] Here $\sigma(\omega, T)$ in our notation is that from MIR and Drude only. Experimentally, this means a cutoff at ω beyond the CT gap.

set free and we are likely left with an $n \propto T$. Actually this variable n finds a common point in the one-component model of $\sigma(\omega, T)$ [38], where renormalized relaxation rate $1/\tau^*$ and renormalized mass m_c^* both depend on T and ω. In other words

$$\sigma(\omega, T) = \frac{ne_c^2}{m_c^*(\omega, T)} \frac{1/\tau^*(\omega, T)}{\omega^2 + [1/\tau^*(\omega, T)]^2}, \tag{7}$$

where n is, however, taken as fixed. In a typical result of this model [39], the renormalized mass $m_c^*(\omega, T)$ at low ω, say 200 cm^{-1}, decreases with increasing T as $m_c^*(\omega, T) = m_{c0}a_0/(a_0 + a_1T)$ with m_{c0} the m_c^* at low T while the renormalized rate $1/\tau^*(\omega, T)$ at low ω roughly increases as T^2. This behavior is perhaps equivalent to an alternative combination of low frequency $n(\omega, T) \propto (a_0 + a_1T)/a_0$ and $1/\tau^*(\omega, T) \propto T^2$ if the mass m_c is taken as fixed instead. Mathematically, by inserting $m_c^*(\omega, T) = m_{c0}a_0/(a_0 + a_1T)$ in equation (7), we have

$$\sigma(\omega, T) = \frac{ne_c^2}{m_{c0}a_0/(a_0 + a_1T)} \frac{1/\tau^*(\omega, T)}{\omega^2 + [1/\tau^*(\omega, T)]^2} \tag{8}$$

$$= \frac{n[(a_0 + a_1T)/a_0]e_c^2}{m_{c0}} \frac{1/\tau^*(\omega, T)}{\omega^2 + [1/\tau^*(\omega, T)]^2}. \tag{9}$$

If we treat mass m_{c0} as fixed, then $n(a_0 + a_1T)/a_0$ can be taken as an effective carrier density which is linear in T, and we arrive at the same conclusion as we made earlier. There must exist renormalization effects to some extent, but meanwhile we cannot rule out the variation of n with T. The problem is, however, that the current optical technique is not able to differentiate one effect from the other because m_c and n are entangled together in the expression of optical conductivity.

Electronic specific heat C^{el} seems to suggest a fixed n because $\gamma = C^{el}/T$ is a constant above T_c [40]. Localized states, as long as they are not far from the Fermi surface ($\sim kT$), nevertheless contribute to γ because these carriers may increase their energy and jump to extended states simply by thermal excitation. Classically this is interpreted as, while being localized and deprived of translational degrees of freedom (DOF), they nevertheless have oscillatory DOF. Thus these states still contribute a term $\propto T$ to C^{el}, such that significant variation in γ/T is not seen. Furthermore, if the states localized are the bound pairs of electron and hole, the pairs as a whole still enjoy a translational degree of freedom and therefore contribute to the specific heat. There are recent reports claiming a scattering rate linear in T shown by ARPES [41, 42]. However, we need to apply caution on the meaning of such a rate and its relation to the actual transport relaxation rate. Averaging to more than 0.2 eV at 300 K [42], such a rate is far above $1/\tau_{tr}$ of 300–500 cm^{-1} given by current IR transport studies. On the other hand, recent dynamic conductivity experiments showed that the T dependence of the transport rate is much faster than T [43], although not really up to a T^2 relation. The THz technique adopted is in principle a much finer probe than ARPES in energy resolution [43], and more importantly, it directly measures the longitudinal transport rate. Similar results are obtained in dynamic optical conductivity experiments [44] at temperatures higher than T_c. The nearly T^2 rate revealed in the THz and dynamic optical experiments could well be the single rate we proposed in this paper.

3. The cause of MIR

A natural question arises as to what contributes to the MIR/midgap (and somehow localized) states. Here we suggest a scenario based on exciton-like interactions. Before delving into details, first we need to clarify the terminology. The term 'exciton', by the usual definition [45], refers to the bound state of an electron–hole pair. It has traditionally been mostly studied in a number of semiconductors since it is convenient to utilize spectroscopic techniques for semiconductor band edges. The electron–hole bound state in a semiconductor is therefore of an excitation nature and short-lived as a consequence. In a semimetal, there are both electrons and holes even in the ground state. The Coulomb interaction between an electron and a hole tends to bind the two into a bound state too. This electron–hole bound state, if formed (by overcoming, say, screening effects), can be naturally referred to as an 'exciton' as well, in the sense of a Coulomb bound state for the electron–hole pair. However, we should keep in mind the semimetal 'exciton' is by no means an excitation of the system. Rather it is a ground-state phenomenon.

In the so-called excitonic pairing model of superconductivity, the term 'excitonic' refers to a charge-transfer type excitation that gives rise to an effective pairing interaction in the earliest Little model. The later models [46, 47] tend to go further, and specifically utilize an excited virtual exciton as the intermediate boson, giving rise to the pairing. Therefore, we should understand that the term 'excitonic' in the case of various superconductivity pairing models typically implies two things: excitation and a Coulomb bound state as in a semiconductor exciton.

Here in this paper, we refer to our model as exciton-like. The term 'exciton-like' is adopted in the strict sense of an electron–hole Coulomb bound state. It should *not* be understood as implying any excitation from the ground state. The semimetal-like band structure of most high-T_c cuprates also rules out the need for an excitation in order to form a Coulomb bound state. This notion can be further understood later when we discuss the stability of the exciton-like bound state in cuprates.

We propose that the peculiar band structure and FS topology near the optimal doping regime, combined with strong Coulomb correlation, contribute to the MIR/midgap states. First, there is strong evidence [24] that electron- and hole-like charge carriers coexist in a broad range of superconducting cuprates, including both the *nominally* n- and p-type. This is a fact probably best born out of recent ARPES experiments [48, 49], and is readily understood from the three-dimensional (3D) Fermi surface topology. For example, to the most rudimentary approximation, LSCO is a hole conductor with a hole-like (h-like) Fermi pocket centered around (π, π). However, such a notion, at the very minimum, neglects the k_z dispersion of the energy band and the associated FS surface topological change. Although the band dispersion along k_z is weak, of the order of 0.1 eV at most, its effect on the FS topology is not trivial [50]. Aggravating the problem is that the ARPES technique currently developed for cuprates is not k_z-sensitive. This contributes to the once much-debated

issue as to whether some salient features represent electron-like (e-like) FS or not [23, 24, 31, 51]. Fortunately, the situation is much clearer now due to much improved ARPES techniques and computational software. Earlier objections [51] to electron-like FS have now shifted to an acknowledgment that such a FS topology exists in a variety of the supposed p-type superconductors [48, 49], at least for certain doping levels.

One commonly asked question is how to reconcile the exciton-like picture proposed here with the well-known antiferromagnetic (AF) correlation existing in the cuprate superconductors. The authors believe that the two pictures do not contradict each other. Rather, they are two facets of the same coin and there should exist causal relationships. It is widely accepted that magnetism is the result of the Coulomb interaction and the Pauli principle. The AF fluctuation is the manifestation of the interaction and the Pauli exclusion in the spin degree of freedom (DOF), while the exciton-like bound state is that in the charge DOF. Both are the results of strong correlations. The Coulomb bound state, for example, is a non-perturbative property and cannot be described by the perturbative expansion of a Coulomb interaction matrix in the form of Feynman diagrams. It is a natural result of strong correlations.

In parallel to the MIR is the widely known pseudogap. There are still many conflicted views on its origin. We believe that a successful theory should be general enough so as to understand all of the above phenomena in a common framework. The interaction between electron-like and hole-like quasiparticles is logical to address such issues.

Electrons and holes attract one another to form weakly bound Mott–Wannier (MW) excitons [45] due to Coulomb interaction. Like that in positronium, the binding energy $E_b = e_c^4 M_\mu / 32\pi^2 \epsilon_0^2 \epsilon_r^2 \hbar^2$ with M_μ the reduced mass and ϵ_0 the vacuum permittivity. The mass of these quasiparticles is of the order of a few m, or the rest mass of a bare electron. In $YBa_2Cu_3O_7$ (YBCO or Y-123), for example, the carrier (e or h) mass $m_c \approx 2m$. [54] The relative dielectric constant $\epsilon_r \approx 14.7$ and thus $E_b \approx 0.063$ eV ≈ 730 K in T [55]. The pseudogap T^* for insulating Y-123 is not known to the author but, for LSCO, $T^* \to 720$ K when the metal–insulator boundary is approached [56]. The good match suggests a possible connection between the exciton-like interaction and a range of puzzling phenomena in cuprate physics.

A common question in the exciton-like scenario is if such a structure is stable against recombination. The lifetime of the often-cited interband (or band edge) exciton in semiconductor physics is much less than one microsecond. The viability of exciton-like bound states in a superconductor therefore might be questioned. We explain that such a concern is not necessary.

3.1. Stability of exciton-like states

Whether electrons (e) and holes (h) should recombine or not depends on the band structure. In semimetals, Bi, As or Sb, for example, e and h coexist without annihilating one another. The reason is as follows and is shown in figure 4.

In typical semiconductors, the conduction and valence bands are separated by a positive energy gap as shown in figure 4(a). By jumping from the conduction to the valence band which is at a lower energy (i.e. recombining with a hole), the thermally excited electron lowers its energy. This process thus occurs spontaneously and annihilates the e–h pair. For semimetals with band configurations typified in figures 4(b) and (c), the situation is, however, totally *different*. If the electron were to jump to the hole state as indicated by the arrows, it would have to take extra energy. This process is clearly unfavored energetically. Such a mechanism secures the stability of the electron–hole liquid against recombination in semimetals. Cuprate superconductors are in a situation similar to semimetals in terms of stability against e–h annihilation. For a superconductor of a single CuO_2 layer, there is a only a single band crossing the Fermi energy. Even in this case, the FS behaves differently (e-or h-like) in its different portions, as we will show in section 3.2.

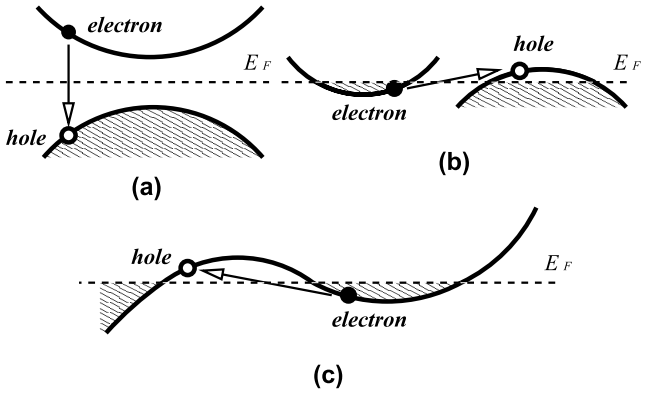

Figure 4. Stability of electron–hole pairs. (a) Typical band structure for semiconductors. Electron states have higher energy than hole states and hence electrons recombine with holes in short time. (b) and (c) Band structure of semimetals. Electron states have lower energy than hole states and the recombination of electrons and holes is unfavored in energy. E_F is the Fermi energy.

3.2. Band structure and FS

To better understand the FS topology, one needs to resort to electronic structure calculation. There have been numerous band structure studies for cuprates. Here we focus on the 3D Fermi surface topology. To the best of the author's knowledge, previous studies largely were on the two-dimensional aspect of FS. For the sake of simplicity, only LSCO will be worked out as an example. The author has explored similar systems such as $Nd_{2-x}Ce_xCuO_4$ (NCCO as e-doped), Bi-2201 and 2212, with characteristically similar results. These studies will appear elsewhere in a separate publication.

Before a detailed discussion on the computational parameters, we need to justify the local density approximation (LDA) approach utilized in the study. It is well known that the LDA band calculation fails to reach the correct ground state for undoped La_2CuO_4. However, once the LSCO is doped beyond the metal–insulator transition [57] (sometimes also called the superconductor–insulator transition, or SIT) point near $x \approx 0.05$, the LDA description of the electronic structure starts to agree reasonably with that of ARPES, as far as the

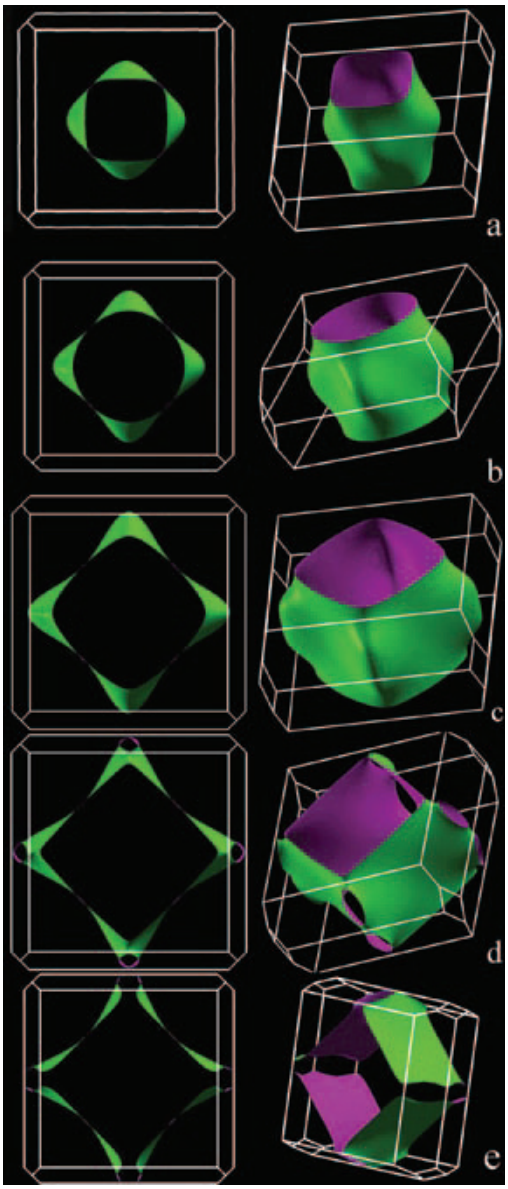

Figure 5. Fermi surface evolution of $La_{2-x}Sr_xCuO_{4-\delta}$ versus decreasing doping level. (a) A theoretical doping of $x \approx 0.4$; (b) $x \approx 0.3$; (c) $x \approx 0.25$; (d) $x \approx 0.16$; (e) $x \approx 0.1$. Green (or the side facing the BZ boundary) indicates the higher energy side of the Fermi surface. Graphs on the left are head-on views from the k_z direction. The three-dimensional views are tilted in different cases to give the best viewing angle. The slight change in the size of the BZ is due to graphic sizing variation.

low energy physics is concerned, such as the electronic states near the Fermi surface. For example, figures 2(a) and (b) of [50] have shown how closely the LDA calculation and the experiment are matched for a fairly underdoped $x = 0.06$. Higher doping tends to give better agreement due to the increasing suppression in the correlation strength, which is also demonstrated in the other parts of figures 1 and 2 in [50]. What we focus on in this paper is the energy scale of up to 0.1 eV within the Fermi energy for doping level $x \geqslant 0.1$ and therefore the LDA and its variations are a good approximation.

The band structure was studied with a first-principles electron structure package [52] utilizing a linearized augmented plane wave (LAPW) basis set. The many-body correlation problem is treated within the framework of local density approximation. Correction due to electron density gradient abides by the general gradient approximation rules and the functional used was that of Perdew–Burke–Ernzerhof. Calculation was carried over 2000 k-points in the first Brillouin zone to ensure a high precision in the resulting band structure and Fermi energy. The **k** vectors were sorted out by their Fermi crossing and plotted in 3D [53].

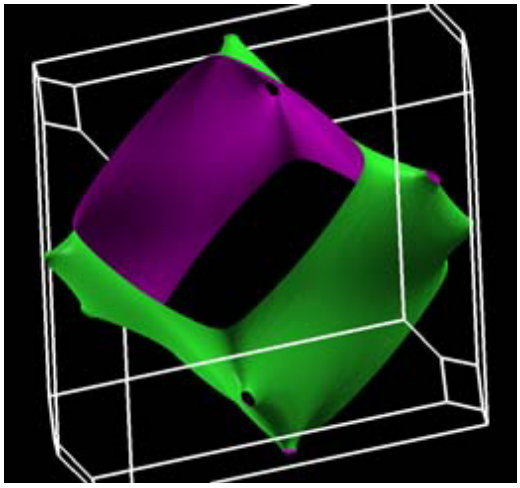

Figure 6. Close-up of the Fermi surface of $La_{2-x}Sr_xCuO_{4-\delta}$ at $x \sim 0.20$. Small necks, 8 in total, open up in the otherwise electron-like portion of FS. These are located on the BZ boundary near $(\pi, 0, \frac{\pi}{2})$ or the equivalent, forming a partly electron-like and partly hole-like Fermi surface. Such a Fermi surface feature corresponds to an energy band straddling the Fermi level near a three-dimensional saddle point. In the extended reciprocal space, such features form the so-called 'jungle gym'.

At a very high but theoretical doping of $x \approx 0.4$ the FS is a mainly an electron tube centered around (π, π). There are portions of the FS that possess some hole-like character, but the absolute portion is very small. With the doping x decreased to ~0.3, the FS section near the basal plane of the first Brillouin zone (BZ) and along the (π, π) direction becomes more h-like. When x is reduced to less than ~0.17, there is a topological change in the FS: a tube or a neck opens up at the BZ boundary, roughly midway between the two planes $k_z = 0$ and π. The detail of the FS at the topological crossover is shown in figure 6.

Figure 5 gives an illustrative explanation as regards to the earlier hesitation in accepting an electron-like Fermi surface in nominally p-type cuprates. At the optimal doping, the Fermi surface is still very hole-like. Previous research tends to focus on 2D segments of FS due to the lack of 3D rendering capability. Schemes depicted in figures 2(a)–(c), and in fact many similar discussions in the literature, actually are built upon a questionable assumption of k_z independence of the Fermi surface. The calculation in figure 5 clearly demonstrates that this is a oversimplification, and often leads to qualitatively false conclusions. Take figure 5(c) for example: the Fermi segment at $k_z = 0$ is already largely hole-like while that at $k_z = \pi$ is still mostly electron-like.

The ARPES techniques that have been developed for high-T_c research are not very sensitive in k_z. As a result, what we have seen for the supposed Fermi surface is merely its 2D projection along the k_z direction. The k_z dependence of the FS near $(\pi/2, \pi/2)$ is negligible. The ARPES FS is therefore strong and unambiguously hole-like near $(\pi/2, \pi/2)$. The situation is complicated at $(\pi, 0)$ due to the relatively strong k_z dependence near the Fermi level. As a result, the ARPES response there is smeared out, forming the often-seen 'shaded' region around $(\pi/2, 0)$, which is interpreted as some sort of unknown state, as that in figure 2(c). Of course, strong correlation further complicates the ARPES spectra, but the long neglected k_z dependence of FS is now becoming recognized.

The near-coincidence of optimal T_c and the topological change demonstrated in figures 5 and 6 does not appear accidental. Actually, if one believes that strong correlations between electron- and hole-like quasiparticles play a role in the superconductivity (SC) mechanism, the coincidence is a logical consequence.

Still, we need prudence so as not to over-generalize. A typical counterpoint is that the neck-like structure exists in ordinary metals, for example copper, yet copper is not superconducting. Possible reasons are as follows. First, too many charge carriers typically reduce the correlation. The Wigner–Seitz radius r_s, which defines the ratio of potential over kinetic energy, scales as $n^{-\frac{1}{2}}$ (2D) or $n^{-\frac{1}{3}}$ (3D). Meanwhile the Coulomb screening increases with charge density n. When the Thomas–Fermi screening strength $q_{tf} \propto (ne^2/E_f)^{1/2}$ is on par with the reciprocal inter-particle distance (roughly given by $1/r_s$), superconductivity tends to disappear. This is actually the general behavior of cuprate superconductors, which lose SC when over-doped. Secondly, the necked FS portion in copper is relatively small compared to the free-electron-like spherical part. To enforce an effective coupling between electrons and holes, the numerical ratio between unlike charges is advantageous near 2–4 to 1. Much higher than 4, a large number of the majority carriers will not be effectively coupled. If the ratio is too close to 1, the system tends to become an excitonic insulator. Thirdly, the cuprate superconductors are strongly two-dimensional which is benign to the formation of bound states due to increased confinement compared to the ordinary three-dimensional metals. Finally, to effect strong electron–hole coupling, the group velocity $\mathbf{v}_g = \nabla_k E_k$ of the relevant carriers need to be close to one another, or near zero. The flat saddle point at $(0, \pi)$ is an ideal harbor for such a coupling.

Therefore the FS topological crossover in SC cuprates appears to significantly amplify the superconducting coupling. This also indicates that a non-traditional pairing mechanism is at play in high-T_c superconductors, and the mechanism is likely exciton-like.

4. Scattering mechanism

All this experimental evidence suggests a promising combination of $1/\tau \propto T^2$ and $n(T) \propto T$ in explaining the peculiar transport in cuprates. Then what is the scattering mechanism behind the T^2 rate? It is likely caused by electron–electron and electron–hole scattering. A fermion–fermion scattering results in a T^2 rate basically because of the phase space restraints from the Pauli principle. In two dimensions (2D), some nesting effect might be prominent but it has been shown that e–e scattering still basically follows a T^2 law [58].

Here we have, however, a variable $n(T)$, which might make us suspect a rate $1/\tau$ increasing faster than T^2. Intuitively the electrons (holes) are getting more crowded with increasing T. So we want to use a very simple argument based on power analysis to show that this worry is not needed.

Treating the scattering process using the Fermi golden rule, the probability per unit time that an electron in $\mathbf{k}$ will be scattered into another $\mathbf{k}'$ is given by

$$w(\mathbf{k}', \mathbf{k}) = \frac{2\pi}{\hbar}\langle \mathbf{k}'|H'|\mathbf{k}\rangle^2 \delta(\varepsilon_{\mathbf{k}} - \varepsilon_{\mathbf{k}'}), \tag{10}$$

where $|\mathbf{k}\rangle = e^{i\mathbf{kr}}$ up to a normalization constant and $H' = e^{-\alpha r}/r$, the screened Coulomb potential. In two dimensions (2D)

$$\langle \mathbf{k}'|H'|\mathbf{k}\rangle = \int \frac{e^{i(\mathbf{k}-\mathbf{k}')\mathbf{r}} e^{-\alpha r}}{r} d^2 r \tag{11}$$

$$= \int \frac{e^{i\mathbf{qr}} e^{-\alpha r}}{r} r\, dr\, d\theta, \tag{12}$$

where $\mathbf{q} = \mathbf{k} - \mathbf{k}'$ and thus $q = 2k\sin(\theta/2)$ with θ the angle between $\mathbf{k}$ and $\mathbf{k}'$.

Notice that, in 2D, $e^{i\mathbf{qr}}$ can be expanded by Bessel functions of the first kind. Then

$$e^{i\mathbf{qr}} = e^{iqr\cos\theta} \tag{13}$$

$$= \sum_{m=-\infty}^{\infty} J_m(qr) i^m e^{im\theta}. \tag{14}$$

Integrate the above first over θ and $e^{im\theta}$ averages to 0 except when $m = 0$. Thus

$$\langle \mathbf{k}'|H'|\mathbf{k}\rangle = 2\pi \int_0^{\infty} J_0(qr) e^{-\alpha r}\, dr = \frac{2\pi}{(q^2+\alpha^2)^{\frac{1}{2}}}. \tag{15}$$

When the screening is not strong, which should be the case for cuprates[6] we see that $\langle \mathbf{k}'|H'|\mathbf{k}\rangle^2 \approx 4\pi^2/q^2 = \pi^2/\sin^2(\theta/2)k^2$, where k will be taken as k_F because effective scatterings only occur near the FS. To be illustrative, we only consider an isotropic case (i.e. the FS is a circle), then the Fermi wavevector $k_F = [2\pi n(T)]^{1/2}$ in 2D where $n(T)$ is taken as the area density of carriers. Without considering the complication from umklapp scattering, we conclude that the transition rate from $\mathbf{k}$ to $\mathbf{k}'$, $w(\mathbf{k}', \mathbf{k})$ is $\propto 1/T$ because $k^2 = k_F^2 \propto n(T)$ and $n(T) \propto T$. Now let us look at the phase space available for scattering. The perimeter of the FS is $2\pi k_F \propto [n(T)]^{1/2} \propto T^{1/2}$ and thus the number of states available for scattering to and from is proportional to the product of the perimeter $2\pi k_F$ and the thermal excitation width $\sim k_B T$ with k_B Boltzmann's constant, in other words proportional to $T^{3/2}$. Applied to both initial and final states this gives us a factor of T^3 from the phase space restriction.

[6] The strong correlation nature of cuprates likely suggests a weak screening.

Combined with a transition probability $w(\mathbf{k}', \mathbf{k}) \propto T^{-1}$, as already seen, it results in a relaxation rate $1/\tau \propto T^2$, which is exactly what we find in experiments. Complications from screening, umklapp process and so on, will be shown in a separate publication but the result is essentially the same.

A similar argument applies to the e–h process where the fermion nature of e and h on their own part gives the same phase restriction we mentioned before and thus the same T dependence for charge transport.

This e–h liquid is perhaps near a Fermi liquid (FL) above the pseudogap temperature T^*. Nonetheless it is not so under T^* because the presence of exciton-like states formed by e and h is significant at low T. These exciton-like pairs are stable against recombination because of the semimetallic band structure, unlike those of the fast-recombining type found in semiconductors. These bound states, as a discontinuous change from the free particle motions, manifest the loss of one-to-one correspondence from the states of the free Fermi gas. This offers an explanation for various non-Fermi-liquid phenomena of cuprates. The importance of discontinuities and non-perturbative approaches in high-T_c superconductivity were very well summarized in [59]. Some 30 years ago, Mott emphasized the interacting nature of such exciton-like states [60]. Kohn [61] and Halperin and Rice [62] pointed out the possible anomalies, like excitonic insulator, CDW, SDW, antiferromagnetic correlation and phase separation, in such a strongly interacting e–h system, which reminds us of many of the correlation phenomena and possibly the stripe phase found in high-T_c materials.

Although Jérome *et al* [63] and Halperin and Rice [62] also argued that the ground state of the excitonic state is an insulator, not to mention superconductivity, their conclusion is *only* true for a system with equal numbers of electrons and holes. If the densities of e and h are not equal, the ground state should be a conductor at least. The possibility of high-T_c superconductivity in systems similar to this was studied by Allender *et al* [46] and Ginzburg [47]. All these suggest a possible connection of high-T_c superconductivity to the exciton-like states of an electron–hole liquid. The authors believe in the value of pairing mechanism studies along the exciton-like model. A preliminary pairing model has been developed, based on quasi-bound states of three electrons and one hole (or alternatively 3h + 1e) [64].

5. Conclusion

This paper is an extension of the authors' previous work as a preprint [65]. At that time, neither electronic structure calculation nor ARPES was sophisticated enough to give precision topology of the Fermi surface. More importantly, only a few researchers challenged the 'conventional wisdom' of the hole-only FS for p-type cuprates. It is worth noting that a large portion of the predictions made in papers [25, 23, 26, 27] and preprints [24, 65] as regards electron-like carriers coexisting with holes is now verified by experiments. At that time the origin of e-like FS was far from clear, and the models were very phenomenological. Still, with a bit of physics insight and careful logical reasoning, we arrived at a conjecture nowadays proved by the ARPES and a number of other experiments.

In summary, we have demonstrated that the puzzling two rates in the normal state can be understood in terms of an effective carrier (quasiparticle) density n almost linear in temperature T and a single relaxation rate nearly $\propto T^2$. This explanation conforms to many experiments although there still exist some problems not fully answered. The variable quasiparticle number has its origin in the midgap localized states, manifested in a number of experiments, for example mid-infrared absorption. Thermal excitation liberates some of the localized carriers, resulting in an n increase with T. We then reason that such a localized state is a logical consequence if the Coulomb correlation between electrons and holes is taken into account, which does not come as a surprise due to the strong correlation in cuprates. The e–h-like quasiparticles form exciton-like bound states, and are therefore localized in their relative coordinates. Semimetal-like electronic structure ensures their stability against recombination. Localized states of the exciton type are only localized in its response to an electric field, therefore hidden where electric response is essential, for example, conductivity and IR conductance. Still, these states have a translational degree of freedom as a neutral particle, therefore contributing to experiments like specific heat and thermal conductance. The exciton-like binding energy, of the order of 0.02 eV, makes the midgap states very close to the Fermi level, further evidence supporting the explanation. Electronic structure calculation was also carried out to explore the 3D topology of the Fermi surface, explaining why there exist e-like carriers in a p-type material, which is also seen in ARPES. The scattering between electrons and holes gives rise to a T^2 dependence in scattering rate, further strengthening the idea of a single rate.

References

[1] Anderson P W 1997 *The Theory of Superconductivity in the High T_c Cuprates* (Princeton, NJ: Princeton University Press)
Anderson P W 1991 *Phys. Rev. Lett.* **67** 2092
Anderson P W 1997 *Phys. Today* **50** (10) 42
[2] Romero D B 1992 *Phys. Rev.* B **46** 8505
[3] Pines D 1994 *Physica* C **235–240** 113
Stojkovic B P and Pines D 1996 *Phys. Rev. Lett.* **76** 811
Stojkovic B P and Pines D 1997 *Phys. Rev.* B **55** 8576
[4] Varma C M *et al* 1989 *Phys. Rev. Lett.* **63** 1996
[5] Hirsch J E and Marsiglio F 1992 *Physica* C **195** 355
[6] Kubo Y and Makano T 1992 *Physica* C **197** 378
Kubo Y and Makano T 1994 *Physica* B **194–196** 2047
[7] Xing D Y and Liu M 1991 *Phys. Rev.* B **43** 3744
[8] Alexandrov A S and Mott N F 1994 *High Temperature Superconductors and Other Superfluids* (London: Taylor and Francis) p 116
[9] Alexandrov A S, Kabanov V V and Mott N F 1996 *Phys. Rev. Lett.* **77** 4796
[10] Levin G A and Quader K F 1996 *Phys. Rev.* B **62** 11879
[11] Gor'kov L P and Teitel'baum G B 2006 *Phys. Rev. Lett.* **97** 240073
[12] Gor'kov L P and Teitel'baum G B 2008 *J. Phys.: Conf. Ser.* **108** 012009
[13] Romero D B *et al* 1992 *Phys. Rev. Lett.* **68** 1590
Gao F *et al* 1993 *Phys. Rev.* B **47** 1036
[14] Quijada M A *et al* 1999 *Phys. Rev.* B **60** 14917
[15] Forro L *et al* 1990 *Phys. Rev. Lett.* **65** 1941

Kamarás K *et al* 1990 *Phys. Rev. Lett.* **64** 84
[16] Michenaud J P and Issi J P 1972 *J. Phys. C: Solid State Phys.* **5** 3061
[17] Alexandrov A S 1996 *Phys. Rev.* B **53** 2863
[18] Ahn C H *et al* 1999 *Science* **284** 1152
Mannhart J, Schlom D G, Bednorz J G and Müller K A 1991 *Phys. Rev. Lett.* **67** 2099
[19] Boebinger G S *et al* 1996 *Phys. Rev. Lett.* **77** 5417
Ono S *et al* 2000 *Phys. Rev. Lett.* **85** 638
[20] Suzuki M 1989 *Phys. Rev.* B **39** 2312
Rice J P, Giapintzakis J, Ginsberg D M and Mochel J M 1991 *Phys. Rev.* B **44** 10158
Forro L *et al* 1990 *Phys. Rev.* B **42** 8704
Tyler A W and Mackenzie A P 1997 *Physica* C **282–287** 1185
Harris J M *et al* 1994 *Phys. Rev.* B **50** 3246
Carrington A *et al* 1994 *Physica* C **234** 1
[21] Shi L *et al* 2005 arXiv:cond-mat/0510794
[22] Hurd C M 1972 *The Hall Effect in Metals and Alloys* (New York: Plenum)
Meaden G T 1965 *Electrical Resistance of Metals* (New York: Plenum)
[23] Luo N 2000 *Physica* C **350** 132
[24] Luo N 2000 arXiv:cond-mat/0003074
[25] Eagles D M 1989 *Solid State Commun.* **69** 229
Eagles D M and Savvides N 1989 *Physica* C **158** 258
[26] Xing D Y and Ting C S 1988 *Phys. Rev.* B **38** 5134
[27] Hirsch J E and Marsiglio F 1991 *Phys. Rev.* B **43** 424
[28] Harris J M *et al* 1995 *Phys. Rev. Lett.* **75** 1391
Kimura T *et al* 1996 *Phys. Rev.* B **53** 8733
[29] Ziman J M 1960 *Electrons and Phonons* (Oxford: Oxford University Press) p 491
[30] Luo N and Miley G H 2002 *Physica* C **371** 259
[31] Chuang Y-D *et al* 1999 *Phys. Rev. Lett.* **83** 3717
[32] Tanner D B and Timusk T 1992 *Physical Properties of High Temperature Superconductors III* ed D M Ginsberg (Singapore: World Scientific) p 363
[33] Timusk T *et al* 1988 *Phys. Rev.* B **38** 6683
Schlesinger Z *et al* 1990 *Phys. Rev.* B **41** 11237
Collins R T *et al* 1989 *Phys. Rev.* B **39** 6571
[34] Uchida S, Eisaki H and Tajima S 1993 *Physica* B **186–188** 975
Uchida S *et al* 1991 *Phys. Rev.* B **43** 7942
[35] Allen J W *et al* 1990 *Phys. Rev. Lett.* **64** 595
van Veenendaal M A, Sawatzky G A and Groen W A 1994 *Phys. Rev.* B **49** 1407
Imada M, Fujimori A and Tokura Y 1998 *Rev. Mod. Phys.* **70** 1039 (see discussion on p 1182 and 1183)
Chen C T *et al* 1991 *Phys. Rev. Lett.* **66** 104
Romberg H M *et al* 1990 *Phys. Rev.* B **42** 8768
[36] Grynberg M, Le Toullec R and Balkanski M 1974 *Phys. Rev.* B **9** 517
[37] Blue M D 1964 *Phys. Rev.* **134** A226
Gurauskas E, Kavaliauskas J, Krivaite G and Sileika A 1983 *Phys. Status Solidi* b **115** 771
Ivanov-Omskii V I *et al* 1970 *Sov. Phys.—Semicond.* **3** 1403
Gerlach E, Grosse P, Rautenberg M and Senske W 1976 *Phys. Status Solidi* b **75** 553
[38] Tanner D B and Timusk T 1992 *Physical Properties of High Temperature Superconductors III* ed D M Ginsberg (Singapore: World Scientific) p 421
[39] Romero D *et al* 1992 *Solid State Commun.* **82** 183
[40] Loram J W, Mirza K A, Cooper J R and Liang W Y 1993 *Phys. Rev. Lett.* **71** 1740
Loram J W, Mirza K A, Liang W Y and Osborne J 1989 *Physica* C **162–164** 498
Mirza K A, Loram J W and Cooper J R 1994 *Physica* C **235–240** 1771
[41] Valla T *et al* 1999 *Science* **285** 2110
[42] Valla T *et al* 2000 *Phys. Rev. Lett.* **85** 828
[43] Corson J *et al* 2000 arXiv:cond-mat/0006027
[44] Kusar P *et al* 2005 *Phys. Rev.* B **72** 014544
[45] Kittel C 1996 *Introduction to Solid State Physics* (New York: Wiley) p 312
[46] Allender D, Bray J and Bardeen J 1973 *Phys. Rev.* B **7** 1020
[47] Ginzburg V L 1970 *Usp. Fiz. Nauk* **101** 185
Ginzburg V L 1970 *Sov. Phys.—Usp.* **13** 335 (Engl. Transl.)
[48] Kaminski A *et al* 2006 *Phys. Rev.* B **73** 174511
[49] Nakayama K *et al* 2006 *Phys. Rev.* B **74** 054505
[50] Sahrakorpi S *et al* 2005 *Phys. Rev. Lett.* **95** 157601
[51] Fretwell H M *et al* 2000 *Phys. Rev. Lett.* **84** 4449
[52] Blaha P *et al* 2001 *WIEN2k, K. Schwarz* Techn. Univ. Wien, Austria
[53] Kokalj A 2003 *Comput. Mater. Sci.* **28** 155
[54] Schlesinger Z *et al* 1991 *Physica* C **185–189** 57
[55] Samara G A, Hammetter W F and Venturini E L 1990 *Phys. Rev.* B **41** 8974
[56] Batlogg B *et al* 1994 *Physica* C **235–240** 130
[57] Damascelli A, Hussain Z and Shen Z-X 2003 *Rev. Mod. Phys.* **75** 473
[58] Fujimoto S, Kohno H and Yamada K 1991 *J. Phys. Soc. Japan* **60** 2721
Maebashi H and Fukuyama H 1998 *J. Phys. Soc. Japan* **67** 242
[59] Anderson P W 2000 *Phys. Today* **53** (2) 11
[60] Mott N F 1961 *Phil. Mag.* **6** 287
Mott N F 1974 *Metal–Insulator Transitions* (London: Taylor and Francis) p 68
[61] Kohn W 1967 *Phys. Rev. Lett.* **19** 439
[62] Halperin B I and Rice T M 1968 *Rev. Mod. Phys.* **40** 755
[63] Jérome D, Rice T M and Kohn W 1967 *Phys. Rev.* **158** 462
[64] Luo N 2001 arXiv:cond-mat/0101004
[65] Luo N 2000 arXiv:cond-mat/0011371